31

Interrelated Analysis of Performance and Fouling Behaviors in Forward Osmosis by Ex-Situ Membrane Characterizations

Coskun Aydiner*, Semra Topcu, Caner Tortop, Ferihan Kuvvet, Didem Ekinci, Nadir Dizge and Bulent Keskinler
Gebze Institute of Technology, Faculty of Engineering, Department of Environmental Engineering, Gebze, Kocaeli, Turkey

1. Introduction

In membrane processes, flux decline takes place as an inherent result of membrane fouling that varies with specificity in their implementations. The membrane fouling having uncontrollable or unexplainable complexity in many cases leads to somewhat loss of process efficiency which results mainly in costly pretreatment, higher operating pressure requirement, limited recoveries, feed water loss, frequent chemical cleaning and short lifetimes of membranes as the factors increasing the water and energy costs (Aydiner, 2010, as cited in Tu et al., 2005; Hoek et al., 2008; Van der Bruggen et al., 2008). In recent years, more economical operation of membrane processes is to be taken into account based on lower energy and membrane costs in practice. At this point, understanding the reasons lying under the fouling phenomena as related with a membrane's performance is to be rather valuable task in terms of scientific and technological developments of these processes (Danis & Aydiner, 2009). However, non-generalization course of the fouling during a membrane filtration necessitates the use of either modeling tools or specific analyses for clarifying meaningful performance-fouling relationships in each specific application. The modeling solutions are widely utilized not only to expose these relations but to put forward performance dynamics intended for a main aim of systematic representation and reasoning. A specific modeling study for lab-scale researches mostly results in simulation deficiencies or key limitations in attainment of a definitive solution when compared to that for real-world implementations. As a matter of fact, the development of simple, accurate and effective models needs to produce a solution relying on a "solution-directed focus" approach which includes full-scale consideration of theoretical and practical issues of the events. But, it is explicit that successive synchronization of model assemblies with real-time could not be entirely accomplished by the community of membrane scientists and technologists at this time. In that sense, it can be said that specific membrane analyses based on either in-situ or ex-situ characterizations could be foreseen as a progressive tool on the purpose of obviating interruption or non-coordination of transition among small and large

* Corresponding Author

scale operations, especially for emerging membrane technologies such as forward osmosis and membrane distillation.

The applications on the membrane fouling characterization falls into two categories: *(i)* laboratory researches involving in-situ monitoring, and *(ii)* field-level studies employing on-line ex-situ scaling observation. In-situ monitoring techniques are to be used for analysing the membrane fouling comprising concentration polarization and cake formation, and are evaluated as an annotation tool in understanding the fouling characteristics (Huang et al., 2010). The most widely used techniques for in situ monitoring of concentration polarization are light deflection techniques (shadowgraphy and refractometry), magnetic resonance imaging, radio isotope labeling, electron diode array microscope, and direct pressure measurements. Whereas, the fouling analyses based on particle deposition or cake layer formation can be carried out by the techniques such as laser triangulometry, optical laser sensor, ultrasonic time-domain reflectometry, electrical impedance spectroscopy, and small-angle neutron scattering (Chen et al., 2004). The main advantage of monitoring-based techniques over traditional lab-scale systems is the ability to visually observe what really happens on the membrane surface simultaneously in real-time (Huang et al., 2010). Ex-situ fouling and scaling detectors are utilized as another important means for understanding of fouling-performance relationships. By the studies under this type of characterization, various observation detectors or fouling simulators can be developed with the intention of controlling the membrane fouling in real-time applications (Uchymiak et al., 2007). Also, various ex-situ membrane investigations based on different analytical techniques such as spectroscopic ellipsometry, x-ray photoelectron spectroscopy (XPS), scanning electron microscope (SEM), atomic force microscope (AFM), Fourier transform infrared (FTIR) spectroscopy, and contact angle etc. can be effectively used for associating the fouling dynamics with the performance (Darton et al., 2004; P. Xu et al., 2010). At the end of a general evaluation of literature on characterizing the membrane fouling, it can be stated that the interrelation of ex-situ characterizations of the membrane fouling concurrently with both process performance and various model response parameters would be a viable simulative tool oriented to removing the transition problems from lab-scale toward real-world. Already, the presence of many techniques and theoretical models developed during the past two decades could makes a sense to better comprehend the interactions between foulants and membrane, develop more viable membranes and employ the process more effectively.

Forward osmosis (FO) is an osmotically–driven membrane process that works spontaneously by osmosis across a semi–permeable membrane. The process possesses a water flow through the membrane from the solution having low concentration (feed solution) toward the solution having high concentration (draw solution) due to the osmotic pressure difference between the solutions (Cath et al., 2006). Along last decade, FO process can be favorably utilized in many applications such as electricity production (Aaberg, 2003; Gormly et al., 2011), power generation (Loeb, 2007; McGinnis et al., 2007), water or wastewater reclamation (Holloway et al., 2007; Cornelissen et al., 2008), seawater desalination or brine concentration (McCutcheon et al., 2006; Low, 2009), concentration of liquid foods (Petrotos & Lazarides, 2001; Dova et al., 2007), protein enrichment and concentration (Yang et al., 2009; Wang et al., 2011), and water purification and reuse in space (Cath et al., 2005a, 2005b). FO process as one of the foremost among processes which have been recently increasingly explored in separation science and technology pursues its

development depending on desalination needs. It has remarkably lower cost due to no hydraulic pressure operation, nearly complete rejection of many contaminants, potentially low membrane fouling tendency (Holloway et al., 2007; Cornelissen et al., 2008; Y. Xu et al., 2010; Wang et al., 2010; Chung et al., 2011). But, there are still some constrains in front of becoming widespread of FO's industrial applications. Major drawback is the lack of a membrane having a relatively high flux compared to commercial reverse osmosis (RO) membranes, as an inherent result of the membrane fouling or internal concentration polarization significantly limiting flux efficiency (McCutcheon et al., 2006; Tang, et al., 2010; Wang et al., 2010). The other is the requirement to provide high osmotic pressure difference under continuously operating conditions in which draw solution needs to be concentrated for producing clean water by a complementary process such as reverse osmosis (RO), membrane distillation, membrane osmotic distillation, decomposition with heating, and magnetic separation (Cath et al., 2005a, 2005b; McCutcheon et al., 2005; Martinetti et al., 2009; Ling et al., 2010).

In spite of its development potential in membrane science and technology, very few publications on the membrane fouling in FO systems were presented in the literature when compared to those in pressure-driven membrane systems. Hence, FO process was especially preferred in this study to interrelate the performance and internal fouling with membrane surface characteristics. Besides, cheese whey was selected as the feed solution due to its high pollutant capacity with rich nutrient content. In order to render the operation of the system as independent of membrane type and operation mode, the process was employed at normal and reverse operation modes using one each of FO and RO membranes. First, the FO system performance was investigated, and internal membrane fouling was estimated by modeling of the performance data. Thereafter, internal fouling was associated with the results of ex–situ membrane surface characterizations. Solute resistivity which is defined as the internal fouling was estimated depending on salt permeability coefficient at the end of the modeling of the performance data. Ex-situ characterizations of the studied membranes were carried out by SEM, AFM, contact angle, and FTIR measurements. Afterwards, the relation equations among external fouling and each one of performance response parameter which comprises of the water flux, specific water fluxes, salt flux, and net and effective osmotic pressure differences were individually evolved by using contact angle determined as illustrative parameter for external fouling from the relation equations among external fouling and internal fouling in ex-situ characterizations. By this way, in light of significant perspectives obtained by joint interpretations of the results, whether or not the membrane fouling can be correlated with the whole performance was put forward. As concluding remarks, the individual mathematical representations of the relationships of internal and external foulings with the performance were elucidated as regards each dynamics of the whole performance. The prospects of more effective treatment of a membrane process were straightforwardly presented in special to osmotically–driven system as independent of membrane type and operating mode.

2. Materials and methods

2.1 Materials

In the experiments, two different membrane materials in a form of flat sheet were used, one being cellulose triacetate (CTA) FO membrane (Hydration Technologies Inc., OR) and the

other being composite polyamide (CPA-3) RO membrane (Hydranautics Inc., CA). FO and RO membranes have salt rejection rates of about 95 and 99.6%, respectively. Their pure water permeabilities, *A* were determined to be approximately 8.1×10^{-3} $m^3/m^2{\cdot}h{\cdot}bar$ and 3.305×10^{-3} $m^3/m^2{\cdot}h{\cdot}bar$, respectively, by means of pure water permeation experiments in a pressure–driven cross–flow membrane system operated at transmembrane pressures of 5, 10, 15, 20 and 25 bar with a constant temperature of 25 °C. FO draw solution used was prepared by dissolving 3 M NaCl (Prolabo, >99%) into the distilled water in order to obtain a high net osmotic pressure difference in the system. Cheese whey was obtained from industrial facilities of Cayirova Milk&Milk Products Inc., located at Kocaeli, Turkey. The characteristics of the raw and FO concentrated cheese whey were presented in Table 1, together with the average water quality values measured in draw solutions after the processing.

parameter	unit	raw cheese whey	FO concentrated cheese whey	FO draw solution
pH		4.97±0.09	4.7±0.1	5.7±1.0
conductivity	mS/cm	6.73±0.08	9.8±3.1	179.8±17.5
Cl^-	mg/L	950±28	1,896±1,103	78,776±10,345
COD	mg/L	58,220±12,509	82,043±30,774	727±905
TOC	mg/L	39,261±2,611	49,013±13,649	30±35
NH_4-N	mg/L	142±8	167±24	2.0±1.1
NO_2-N	mg/L	0.04±0.02	0.2±0.2	0
NO_3-N	mg/L	254±15	280±34	0
TKN	mg/L	1,353±139	1,659±343	6.1±5.6
Org-N	mg/L	1,211±138	1,492±321	4.1±6.0
TN	mg/L	1,607±146	1,939±371	6.1±5.6
PO_4-P	mg/L	370±10	464±116	7.3±13.3
TP	mg/L	470±98	569±154	12.6±23.0
total protein	%	2.38±0.18	3.23±1.16	–
fat	%	0.37±0.07	0.50±0.12	–
SNF (fat–free dry matter)	%	6.39±0.22	8.82±3.04	–
total solid content	%	6.76±0.29	9.32±3.14	–
lactose	%	3.05±0.27	4.48±1.61	–
minerals	%	0.99±0.06	1.39±0.42	–

Table 1. Characteristics of the raw and FO concentrated cheese whey and the average water quality observed in draw solutions

It should be noted in Table 1 that COD and TOC parameters were measured as soluble COD and soluble TOC in cheese whey samples, and dash means that the relevant parameters were not measured in draw solution samples.

2.2 Methods

2.2.1 Experimental procedure

The experiments were carried out by a lab–scale FO system shown in Fig. 1. The process was operated in both normal and reverse orientation mode with a closed loop, which means

that the active or selective layer of the membrane was faced on draw solution and whey, respectively. Cross–flow membrane module was a custom made cell with equivalent flow channel at both sides of the membrane. The membrane module which was made from Delrin acetal resin material (DuPont, Wilmington, Delaware) has an effective membrane area of 140 cm^2. The system was employed with 3 L volumes for both the feed (whey) and draw sides. Hydrodynamic flow at the channels was co–currently run to reduce strain on the suspended membrane. Two speed controllable peristaltic pumps (EW 77111–67, Cole Parmer, IL) were used to pump whey liquor and draw solution. Cross–flow velocities on both faces of the membrane were kept constant with 5 L/min (0.5 m/s). The setup was also equipped with a constant temperature water bath (462–7028, VWR Scientific, IL) to maintain the same temperature (25±0.5 ^oC) at both solutions during FO tests. Each experiment was conducted with 360 min duration time.

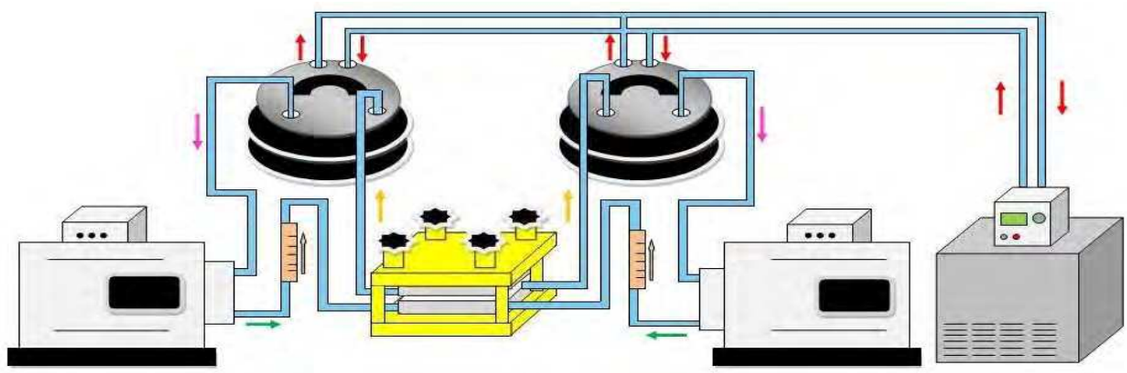

Fig. 1. Experimental setup of lab-scale FO system

2.2.2 Analytical procedure

Total protein, fat, fat–free dry matter (SNF), total solids, lactose and minerals contents of cheese whey samples were measured by Lactostar instrument equipped with thermal and optic sensors (Funke Gerber Company, Germany). The pH, conductivity, and temperature measurements were done by using WTW Multi 340i Meter (WTW, Weilheim, Germany). For density measurements in the samples, DA–130N density meter (KEM Co., Ltd., Kyoto, Japan) was used. Osmolalities of the samples were determined in duplicate for each data point by Advanced Osmometer instrument (Model 3250–Advanced Instruments Inc., USA) in accordance with freezing point depression method after completing the entire experiment. The analyses of water qualities in whey and draw solution were carried out in accordance with standard methods (American Public Health Association, 2005). Besides, nitrite, nitrate, and TOC, TN parameters were analyzed using GBC UV–visible Cintra 20 spectrometer (Cintra, Australia), and HACH IL 550 TOC–TN (Hach Lange Ltd., Germany) instruments, respectively.

2.2.3 FO performance calculations

The permeated water volume, V was determined from the osmolality differences of both solutions. First, the osmolalities of solutions were individually measured at definite time intervals along the experiments, and thereafter V was determined from the differences of

sequential time points by calculations on osmolarity–based mass balance. These results were also made valid by their verification from time–dependent variations of total solid content (*TSC*) of cheese whey in the feed. The water flux, J_w was determined from the volume increase in the draw solution using Eq. (1).

$$J_w = \frac{1}{A_m} \cdot \frac{\Delta V_t}{\Delta t} \tag{1}$$

where A_m is the membrane area, t the time, and V_t the volumetric water permeation at any time. The salt flux, J_s flowed in reverse direction from the water flux between both solutions was calculated using the following equation (Cornelissen et al., 2008).

$$J_S = \frac{1}{A_m} \cdot \frac{\Delta(C_t \cdot V_t)}{\Delta t} \tag{2}$$

where C_t is the salt concentration at any time. In addition to J_w and J_s, the specific water fluxes as the water flux per net osmotic pressure difference (J_w'), and the water flux per net osmotic pressure difference normalized with respect to the osmotic pressure of the feed solution (J_w^*) were also calculated from Eqs. (3), and (4), respectively.

$$J_w' = \frac{J_w}{\Delta\pi_{net}} \tag{3}$$

$$J_w^* = \frac{J_w \cdot \pi_{f,b}}{\Delta\pi_{net}} \tag{4}$$

Time–dependent variations of two osmotically–driven forces comprising net osmotic pressure difference ($\Delta\pi_{net}$) and effective osmotic pressure difference ($\Delta\pi_{eff}$) were examined for various operating conditions. The net osmotic pressure refers to the osmotic pressure difference between the draw and feed solutions in the system. It was determined from difference of osmotic pressures of both solutions after analytically measurement of each solution osmolality by (Cornelissen et al., 2008; Tan & Ng, 2008)

$$\Delta\pi_{net} = \pi_{d,b} - \pi_{f,b} \tag{5}$$

where $\pi_{d,b}$ and $\pi_{f,b}$ are the osmotic pressures of the draw and feed solutions, respectively. The osmotic pressures in the solutions were calculated in accordance with the van't Hoff equation.

$$\pi = R \cdot T \cdot [\ m \ \cdot \ d\ ] = R \cdot T \cdot [\ i \cdot C\ ] \tag{6}$$

where R is the ideal gas constant (8.314 J/K·mol), T the absolute temperature (K), m the osmolality (mosm/kg), d the solution density (kg/L), i the van't Hoff factor, and C the molar concentration. It should be noted that the multiplication term in square bracket at left–hand side is referred to as the osmolarity (mosm/L) representing total solute concentration in the solution. The equivalence on the left–hand side of the equation was used to determine the osmotic pressure of the draw solution during the experiments. Whereas, the equivalence on

the right–hand side was utilized for obtaining theoretical salt permeability coefficient in frame of the model calculations (see the section 2.2.4).

The effective osmotic pressure is the principal driven force that essentially governs osmotic water permeation into the draw solution. It takes place as an inherent event of internal concentration polarization which forms the most significant portion of the whole membrane fouling. It is theoretically predicted from the difference of osmotic pressures at the draw and feed sides of membrane's active layer using Eq. (7), as independent of the membrane operation mode (Tan & Ng, 2008).

$$\Delta\pi_{eff} = \pi_{d,w} - \pi_{f,w} \tag{7}$$

2.2.4 Modeling framework

The water flux, J_w is represented as a function of the effective osmotic pressure difference according to the osmotic–pressure model given as (Cornelissen et al., 2008; Tan & Ng, 2008)

$$J_w = A \cdot (\pi_{d,w} - \pi_{f,w}) \tag{8}$$

where A is the pure water permeability of the membrane. In the process, another flux term needs to be taken into account due to salt transport taking place simultaneously with water transport. Dissolved salt ions transport from the draw toward the feed, as being in reverse direction to the water flow. It should be designated that mutually transport dynamics goes on across the selective layer of the membrane until system reaches equilibrium. This second flux parameter known to be the salt flux, J_s is determined by Eq. (9) (Cornelissen et al., 2008; Tan & Ng, 2008).

$$J_s = B \cdot (C_{d,w} - C_{f,w}) \tag{9}$$

The modeling of FO process is widely carried out based on water flux from the osmotic pressure difference among the draw and feed solutions which is usually theoretically determined using the data obtained from the experiments. In an osmotically–driven membrane process, water and solute transport in a membrane matrix takes place across a selective interface inside the membrane by convection and diffusion. The fouling phenomena in the membrane become together simultaneously with the transport events, in which two distinctive behaviors known as internal and external concentration polarizations occurs inside and outside the matrix, respectively. The restrictiveness of the fouling on the process efficiency comes from its weakening effect on the effective osmotic pressure of which internal fouling portion plays dominant role. Hence, the main subject in assessing the process performance by the modeling is to be the molar salt concentrations at both sides of the membrane wall which are admitted as a key factor for driven force (Cath et al., 2006; McCutcheon & Elimelech 2006). But, different operation modes (normal and reverse modes) of FO process lead to quite differentiation of the effect of internal concentration polarization depending on the placement of the membrane's active layer toward the draw or feed solution. In a FO process being operated at normal mode in which membrane's selective layer is faced on the draw solution, concentrative internal concentration polarization is valid. Whereas, at reverse mode which means that the selective layer faced on the feed solution, dilutive concentration polarization governs the process. As the indicator of internal

membrane fouling, solute resistivity resulted from soluble concomitant ions inside the active layer can be estimated by Eqs. (10), and (11), respectively (Loeb et al. 1997; Cath et al., 2006; McCutcheon & Elimelech 2006).

$$K = \left(\frac{1}{J_w}\right) \cdot \left[\ln\left(\frac{B + A \cdot \pi_{d,w} - J_w}{B + A \cdot \pi_{f,b}}\right)\right] \tag{10}$$

$$K = \left(\frac{1}{J_w}\right) \cdot \left[\ln\left(\frac{B + A \cdot \pi_{d,b}}{B + J_w + A \cdot \pi_{f,w}}\right)\right] \tag{11}$$

In accordance all the equations given above for performance and fouling, performance data related to the water and salt fluxes were simultaneously modeled as a result of which actual internal membrane fouling was defined as solute resistivity at the scope of computational methodology briefly outlined in Fig. 2. The modeling was based upon a framework rendering time–dependent estimation of FO data that was individually fulfilled for each selected time point of each time–dependent data set obtained experimentally. In the computations, theoretical salt permeability coefficient, $B_{\text{theoretical}}$ was determined using Eq. (12) which is obtained by the equalization of Eqs. (8), and (9), together with the use of the formula on right–hand side of Eq. (6).

$$B = \frac{-J_s \cdot i \cdot A \cdot R \cdot T}{J_w} \tag{12}$$

Osmotic pressures at the membrane's wall were predicted using π–C relationship given in Eq. (13) which was determined experimentally for NaCl solution up to 4 M concentration.

$$[\pi] = (5.8062 \times C^2) + (40.091 \times C) + 0.7289 \quad (r^2=1.000) \tag{13}$$

2.2.5 Ex-situ membrane characterizations

Ex-situ membrane investigations were carried out with the surface characterizations of active and support layers of the studied membranes by SEM, AFM, FTIR, and contact angle. Prior to analytical measurements, representative samples were washed twice with pure water and dried at room temperature. The views of membrane's active and support layers were observed by AFM (NanoScope IV AFM) and SEM (Philips XL30 SFEG). The membrane surface roughness was measured in contact mode by AFM. The mean surface roughness (R_A), the root mean square error (R_{RMSE}) of the average height of surface peaks, and the mean difference in height among the five highest peaks and the five lowest valleys (R_Z) were established to compare the roughnesses of FO and RO membranes depending on the membrane fouling. After Au coating of the samples, SEM images were taken at 5 kV to view the surface fouling. The contact angle was measured using a goniometry instrument (KSV Instruments, CAM 101) as an indicator for the hydrophilicity or wettability of the membrane surfaces. In the analysis, 2 μL of pure water in a tight syringe was dropped on the surface according to the sessile–drop technique. The results were obtained as the average values of contact angles at both sides of each drop fall on four arbitrary places of the samples. FTIR technique was employed to examine the interactions between whey components with the

active and support layers of the membranes studied, respectively. The infrared spectra were recorded in a wave number range of 4000–650 cm^{-1} on a Bio Rad FTS 175C spectrophotometer.

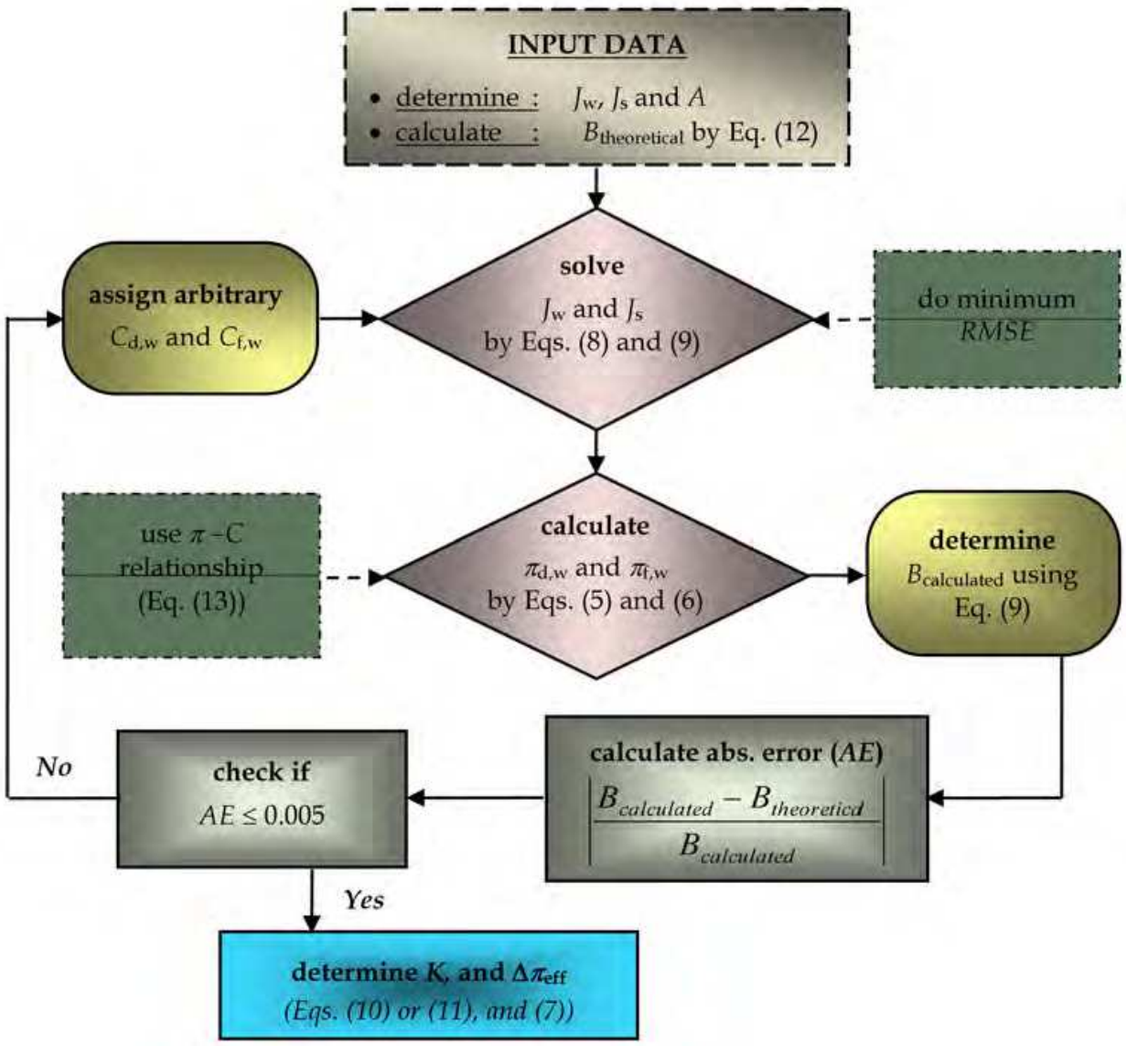

Fig. 2. Computational methodology used in the modeling of experimental data

3. Results and discussion

3.1 Analysis of FO Performance

3.1.1 Water permeation and fluxes

Time-dependent variations of water permeation and both fluxes depending on two different operation modes of both membranes were depicted in Fig. 3. In the figure, dotted lines are the results estimated from the modeling of experimental water and salt fluxes, whereas solid lines are the non-linear fitting curves for water permeation.

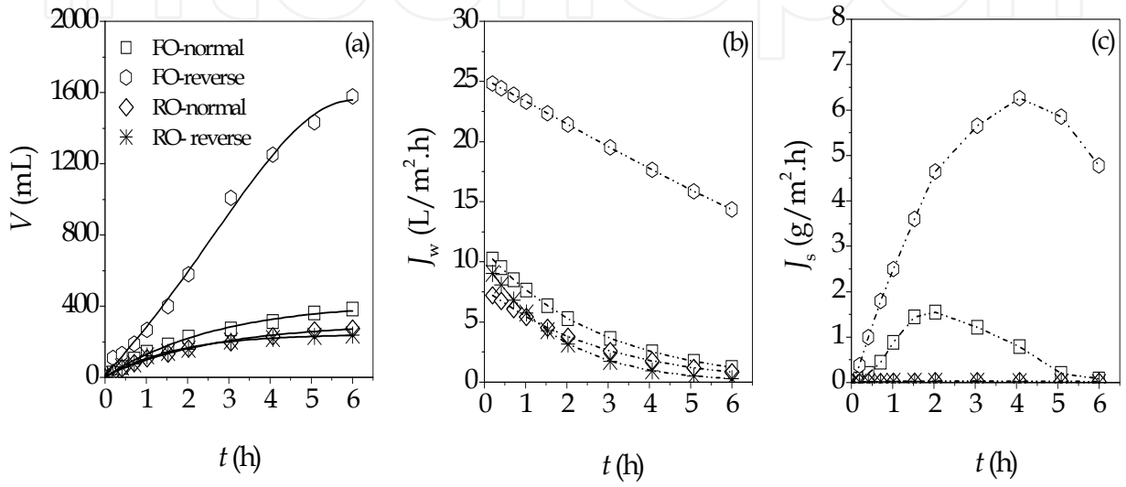

Fig. 3. FO performance at normal and reverse modes for both membranes ((a) volumetric water permeation, (b) water flux, and (c) salt flux)

The process instituted rather different performances at the conditions operated with FO and RO membranes. The system reached a steady state at the end of 360 min except for FO-reverse condition. A conspicuous superiority for reverse operation mode of FO membrane in whey concentration was established in which water more than half of initial water volume of whey was withdrawn as being approximately five times higher than other three varieties. But, FO membrane performed lower salt rejections due to relatively higher salt passages into the whey. It can be accordingly said that novel FO membranes need to be developed to remove the partial deficiency in rejecting salt ions as well as to allow higher water flux performance when also compared to those of RO membrane systems.

3.1.2 Driven forces, *B* and *K* variations

The effective osmotic pressure difference, salt permeability coefficient and solute resistivity were estimated by means of the model calculations based on computational methodology of experimental data presented in Fig. 2. Time evolutions of the estimated parameters via net driven force determined experimentally were presented in Fig. 4. In the figure, solid lines are the non-linear fitting curves, while dotted lines and symbols are the calculated and theoretical values of B, respectively.

In the process, net driven force decreased in company with the amount of water permeated into the draw solution. Quite different time variations were observed for the model parameters. FO membrane exhibited relatively higher salt permeability even at normal mode depending mainly on higher salt flux compared to that of RO membrane. Figs. 3-(a) and 4-(d) clearly indicated that the water flux performance of the process occurred as an inherent consequence of concentrative or dilutive concentration polarization influence of the membrane's active layer in different operation modes. Despite higher salt passages, FO membrane's inner was fouled less than RO membrane's by organic and inorganic solutes. These results gave some hints on the development of novel FO membranes. So, a FO membrane should preferably be as much thinly as possible designed by enabling high rejection rates especially for monovalent solutes and low molecular weight dissolved organics. In that circumstance, more effective operation of the FO system can be anticipated in terms of the operability with a longer period of time at high performance levels under the influence of lower internal fouling.

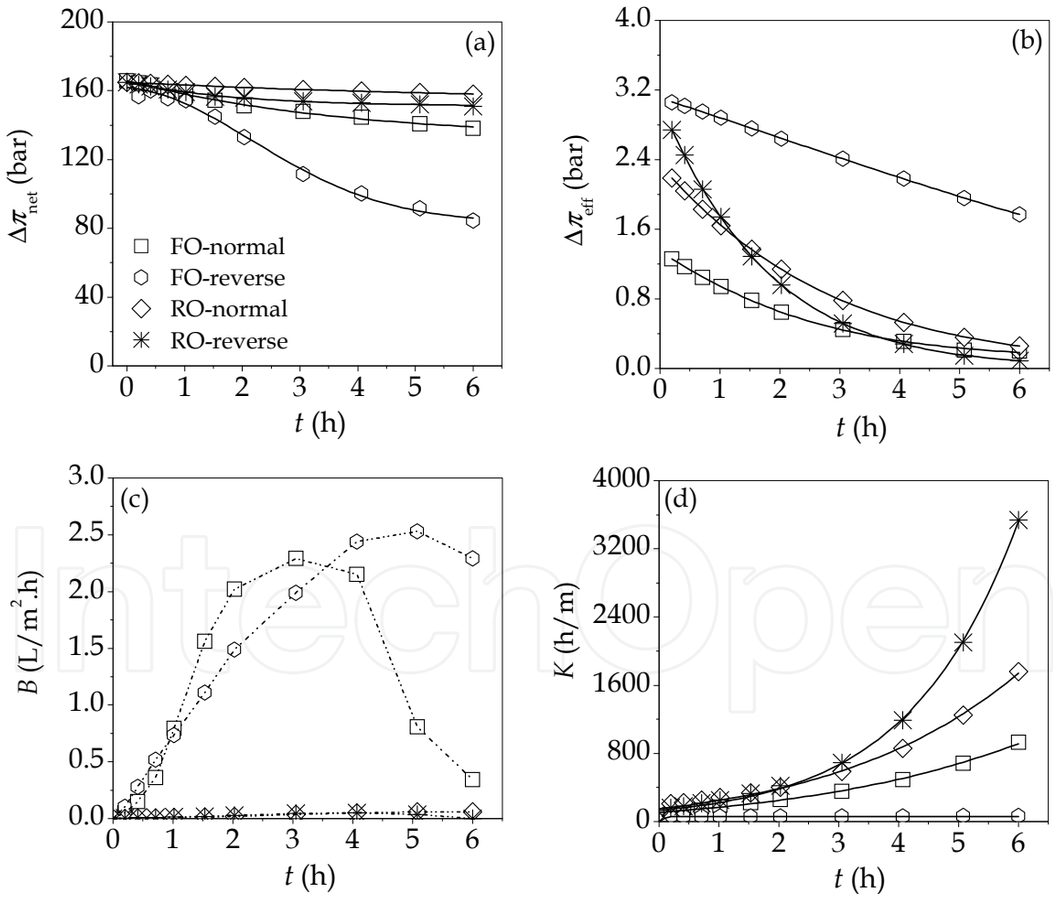

Fig. 4. Results for three modeling parameters via net driven force ((a) net osmotic pressure difference, (b) effective osmotic pressure difference, (c) salt permeability coefficient, and (d) solute resistivity)

3.2 Evaluation of ex-situ fouling

3.2.1 AFM, SEM and contact angle

Visual inspection of a membrane are employed by micro- or nano-scale membrane autopsy in which some properties such as microstructure and morphology can be observed to find any physical damage or changing on the surface. By means of analyses based on these observations, significant information are obtained with the intents of determining the membrane characteristics, analyzing the intensity or course of the membrane fouling, and improving the membrane properties for obtaining better performance. In that sense, top view AFM and SEM images of the surfaces of the studied membranes were shown in Figs. 5 and 6 for the active and support layers, respectively. In addition, contact angle and roughness results measured on the membrane surfaces were presented in Table 2.

membran–mode	active layer				support layer			
	θ°	R_A (nm)	R_Z (nm)	R_{RMSE} (nm)	θ°	R_A (nm)	R_Z (nm)	R_{RMSE} (nm)
FO clean	67.9±10.7	2.2	3.4	12.5	93.5±4.0	2.8	3.6	12.8
RO clean	62.5±2.9	30.1	50.2	191.6	43.0±8.1	74.5	93.4	368.2
FO–normal	43.8±12.4	19.8	30.6	103.1	61.5±3.4	30.1	35.2	115.4
FO–reverse	50.0±2.3	58.4	76.0	258.7	64.5±14.2	23.9	32.3	125.8
RO–normal	43.5±10.8	96.1	116.8	425.8	68.0±5.8	9.7	14.5	42.0
RO–reverse	41.3±17.8	76.2	96.6	326.9	72.8±4.9	36.8	44.8	181.7

Table 2. Contact angle (θ°) and roughness (R, nm) of the active and support surfaces of FO and RO membranes

Table 2 indicates the general fouling trends in the FO system including organic and inorganic foulants on each opposite side as independent of orientation mode of the membranes. As can be seen from Figs. 5 and 6 and Table 2, RO membrane was fouled more intensively, and wettability and roughness on the active surface of both membranes increased. However, higher increasing rates in external fouling of FO membrane were observed as more than those of RO membrane. Wettability and roughness increased on the support layer of FO membrane, whereas decreased on the support layer of RO membrane in spite of increased fouling. AFM and SEM images and contact angle results pointed out that the surface foulings formed on the layers of FO and RO membranes resulted from different fouling dynamics depending on solute-membrane and solute-solute interactions.

3.2.2 FTIR Spectra

FTIR technique is widely used to characterize functional groups on a membrane surface via attenuated total reflection (ATR). As is known, organic and inorganic compounds absorb the infrared radiation energy corresponding to the vibrational energy of atomic bonds. By this unique property in the absorption spectrum, the functional groups of a specific compound can be identified by means of FTIR spectra. Hence, the variations of functional chemistry on both surfaces of FO and RO membranes were investigated by FTIR spectroscopy, and thereby general behaviors in the membrane fouling were comparatively evaluated.

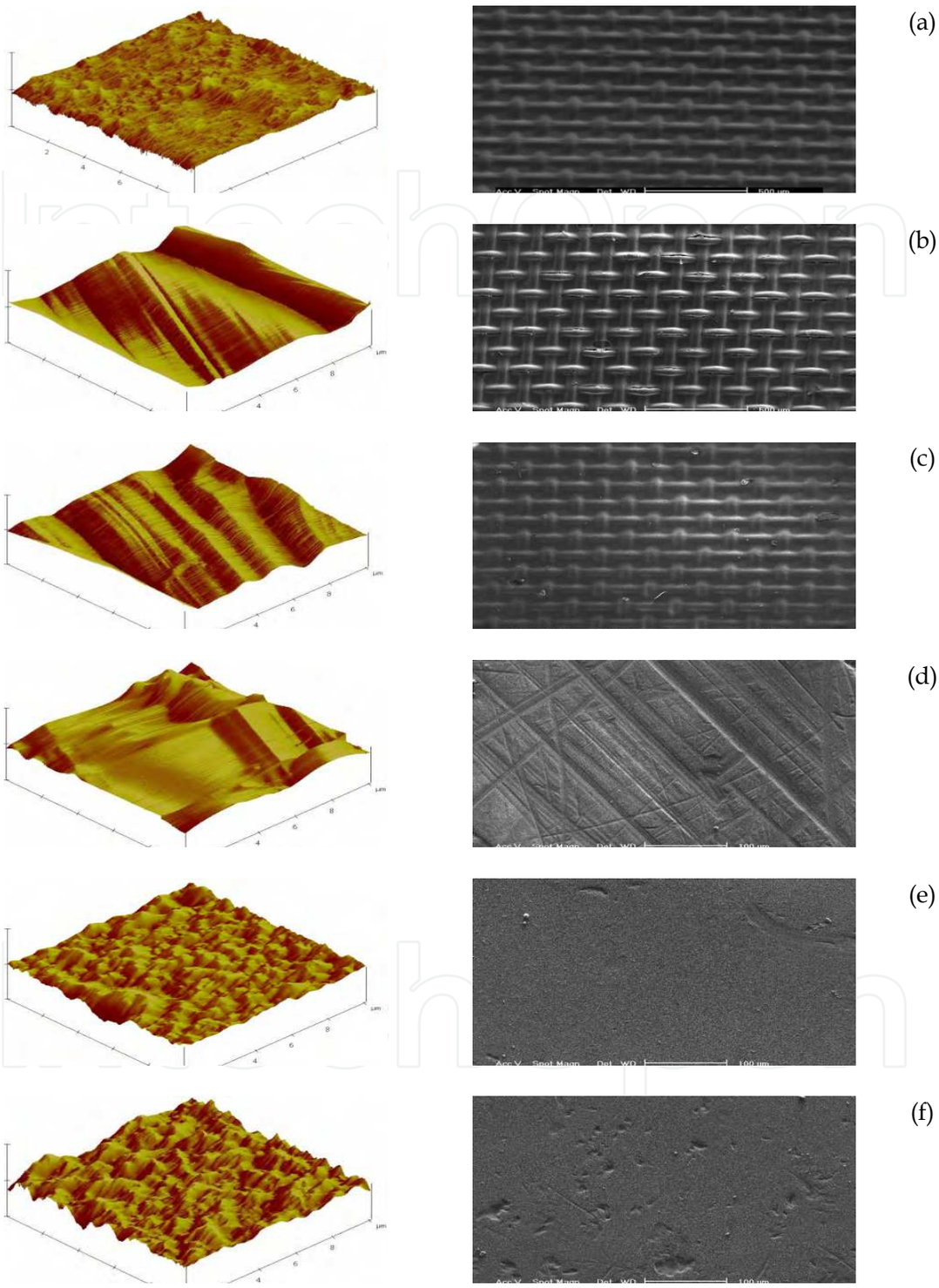

Fig. 5. Top view AFM images and SEM microphotographs of active layer of clean and fouled membranes ((a) FO clean, (b) FO–normal, (c) FO–reverse, (d) RO clean, (e) RO–normal, and (f) RO–reverse)

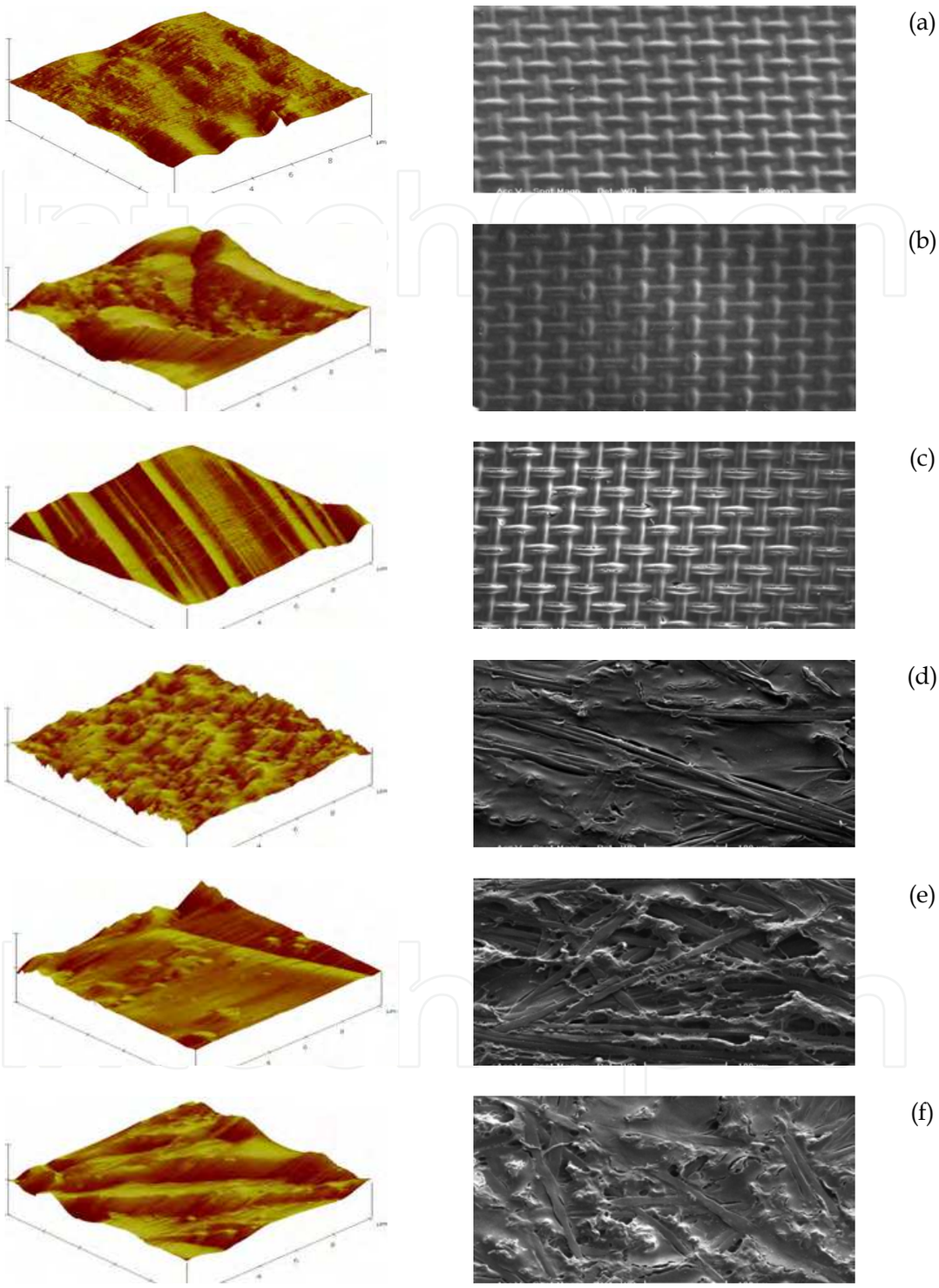

Fig. 6. Top view AFM images and SEM microphotographs of support layer of clean and fouled membranes ((a) FO clean, (b) FO–normal, (c) FO–reverse, (d) RO clean, (e) RO–normal, and (f) RO–reverse)

To determine surface groups responsible for external fouling, the results obtained by FTIR analyses were depicted in Figs. 7 and 8 for active and support layers of the studied membranes, respectively. In FTIR spectroscopy, whey containing rather different chemical groups absorbs infrared radiation energy at different band levels. Absorption bands at 1600–1700 and 1520–1565 cm^{-1} are responsible for amide I and amide II groups of protein structures, respectively. Besides, the bands at 1725–1745 and 1400–800 cm^{-1} are assigned to C–O stretching of fats, and coupled stretching and bending of carbohydrates, respectively. The vibration bands of clean FO membrane at 1730–1745, 1370–1390, 1235–1245, 1040–1100, and 880–995 cm^{-1} were possibly indicative for C=O stretching of carboxylic acid, symmetric CH_3 bending, C–O stretching, C–O stretching of carboxylic acid or C–N stretching, and asymmetric =C–H or $=CH_2$ stretching, respectively. Whereas, those of clean RO membrane at 1630–1680, 1500–1600, 1485, and 1040–1100 cm^{-1} were attributed to the stretchings of C=C, C=C ring, CH_2, and C–O, respectively. The bands at around 3445 and 3272 cm^{-1} corresponded to asymmetric and symmetric O–H stretching of water molecules on the surface due to deficient drying of the samples. As independent of membrane operation mode, lower transmission intensities on the surfaces of RO membrane indicated more severe fouling than those of FO membrane. It was also ascertained that similar transmission peaks corresponded to comparable foulings on the surfaces of both membranes. All of the peaks extended to a range of 700-1750 cm^{-1} proved that the surfaces of both membranes were fouled by severe adsorption of proteins, lactose and fats in whey.

3.3 Interrelated analysis of performance and fouling

3.3.1 Modeling-based approach

This approach, namely "*modeling-based performance analysis*" was focused on the membrane fouling results obtained by the modeling of the performance results. Herein, internal fouling-performance relationships can be explicitly derived with mathematical equations as related to two different groups of performance parameters, one being the measurable parameters ($\Delta\pi_{net}$, J_w and J_s), and the other being the prevailing estimated parameters ($\Delta\pi_{eff}$, J_w^* and B). At the basis of the membrane solute resistivity, non-linear relationships were evolved according to the statistical power law analysis. The equations belonging to data set at the end of the process were shown in Eqs. (14), and (15), while those belonging to the whole time–dependent data set were given in Eqs. (16) and (17). In these equations, internal fouling was represented separately for the measurable and the prevailing estimated responses. Standard error of estimate (S) and correlation (r^2) were also presented.

$$K_m = (0.00091)\cdot\left[\Delta\pi_{net}\right]^{2.780}\cdot\left[J_w\right]^{-0.368}\cdot\left[J_s\right]^{-0.083} \quad (r^2=1.000) \tag{14}$$

$$K_{pe} = (192.4)\cdot\left[\Delta\pi_{eff}\right]^{0.018}\cdot\left[J_w^*\right]^{-0.810}\cdot\left[B\right]^{0.028} \quad (r^2=1.000) \tag{15}$$

$$K_m = (0.127)\cdot\left[\Delta\pi_{net}\right]^{1.836}\cdot\left[J_w\right]^{-0.919}\cdot\left[J_s\right]^{0.015} \quad (r^2=0.993;\ S=60.3) \tag{16}$$

$$K_{pe} = (132.7)\cdot\left[\Delta\pi_{eff}\right]^{-0.121}\cdot\left[J_w^*\right]^{-0.779}\cdot\left[B\right]^{0.017} \quad (r^2=0.989;\ S=73.0) \tag{17}$$

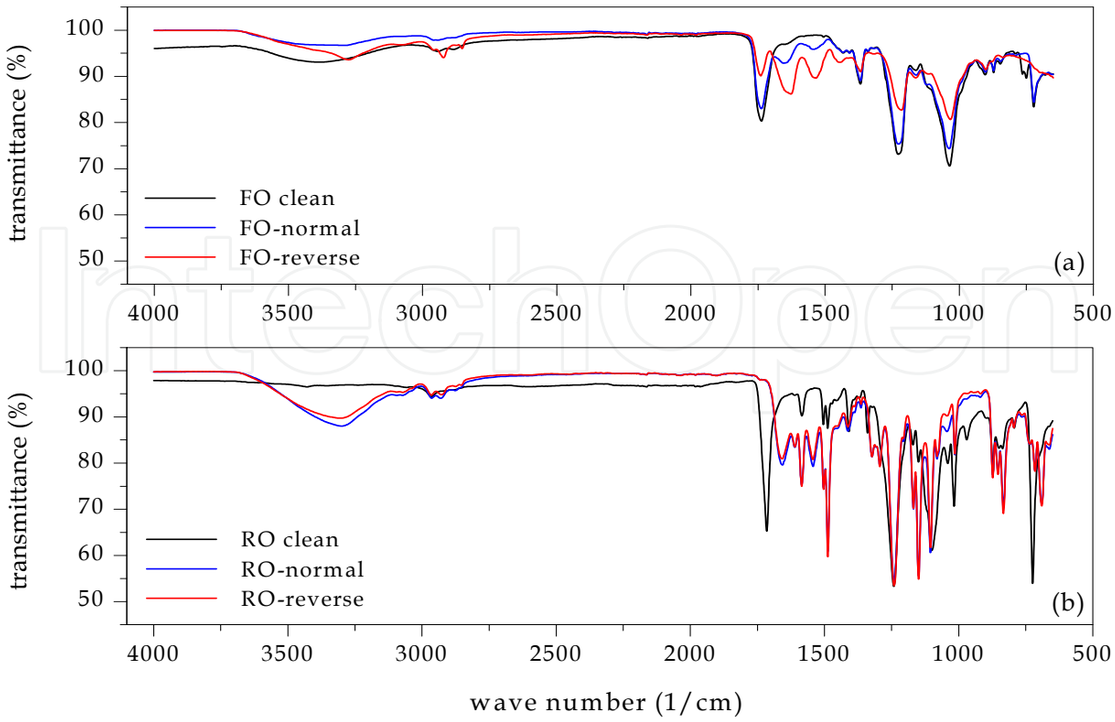

Fig. 7. FTIR spectra of active layers of FO (a) and RO (b) membranes

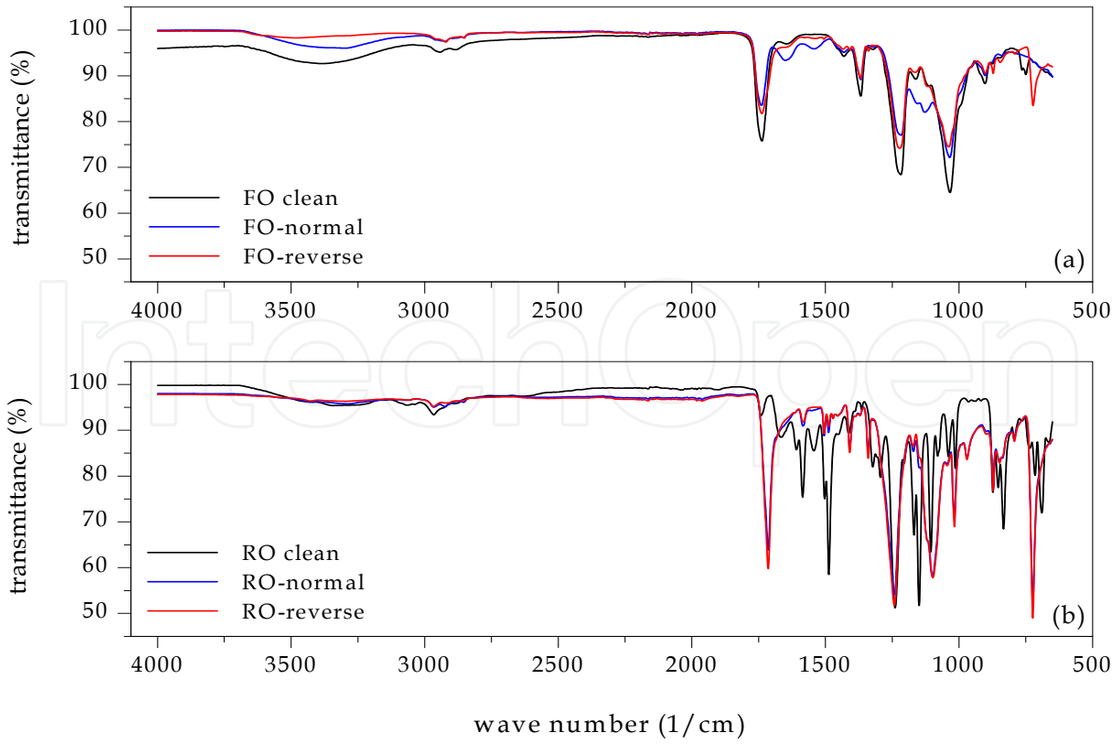

Fig. 8. FTIR spectra of support layers of FO (a) and RO (b) membranes

Eqs. (14)-(17) proved that internal fouling was remarkably interrelated one by one with both groups of the performance variables. The internal fouling estimates were considerably reliable for simulating the FO performance due to very good agreements. With respect to final performances, the internal fouling increased by increasing of driven forces and salt permeability, while decreased by increasing of water and salt fluxes. The major restricting factor for the performance distinctly seemed to be net pressure difference. Water and salt fluxes were determined to be the second and the third factors in the system efficiency, respectively. According to these results, a FO process has to be employed with a draw solution to be yielded high net driven force. It should be however emphasized that this choice would not be alone sufficient for the expected efficacy in practice. Furthermore, the modeling-based analysis indisputably revealed that the membranes to be specifically designed with the intents of higher driven forces and lower salt permeability would be able to be operated with enough high performances. In other words, a FO membrane having a high salt rejection (>99%) under relatively high effective driven force would be effectively utilized by higher clean water production rates even under a reasonable net driven force.

3.3.2 Ex-situ-based approach

Ex-situ-based approach can be described as "*ex-situ membrane characterization-based performance analysis*" of which the methodology is principally relied on an illustrative surface parameter to be representative for the internal membrane fouling. The approach follows a solution-directed strategy that includes a focal point toward predicting each performance component as associated individually with representative surface parameter. Accordingly, firstly roughness and contact angle of the membrane surfaces were associated with the internal fouling by appropriate one of linear and non-linear curve-fitting techniques to be given the highest correlation for the relation equations. Thereafter, each performance parameter was related to contact angle determined as representative for the internal fouling.

The best relationships obtained in the first step of ex-situ-based performance analysis were shown in Fig. 9. The surface morphologies of the fouled membranes did not give meaningful correlations for which belong to the membrane surface coated by foulants not to the membrane itself. Unlike this case, wettability of both surfaces of FO and RO membranes were relevant to the internal fouling. However, a high correlation of r^2=0.985 could only be obtained for the wettability of the active surface. This meant that the internal fouling was directly related with the hydrophilicity of the active layer, but not with that of the support layer. Fig. 9-(b) also showed that wettability of the active surface increased as internal fouling increased. Accordingly, internal and external foulings were interrelated with each other by the relation equations. More importantly, the increase in external fouling concurrently led to the increasing of internal fouling. Thereupon, it can be said that a novel FO membrane should be designed in a form of enabling less external fouling on its active surface without compromising the compatibility with net driven force.

At the second step of the approach, contact angles of the surfaces were interrelated to the performance responses comprising osmotically–driven forces, salt and water passages, and the results were depicted in Figs. 10, 11, and 12, respectively. Equating procedure of wettability of the support layer was determined as practically rather complex of which the relations performed distribution-type variations. Thus, performance simulations were relied on the wettability of the active layer possessed good agreements with the experimental data.

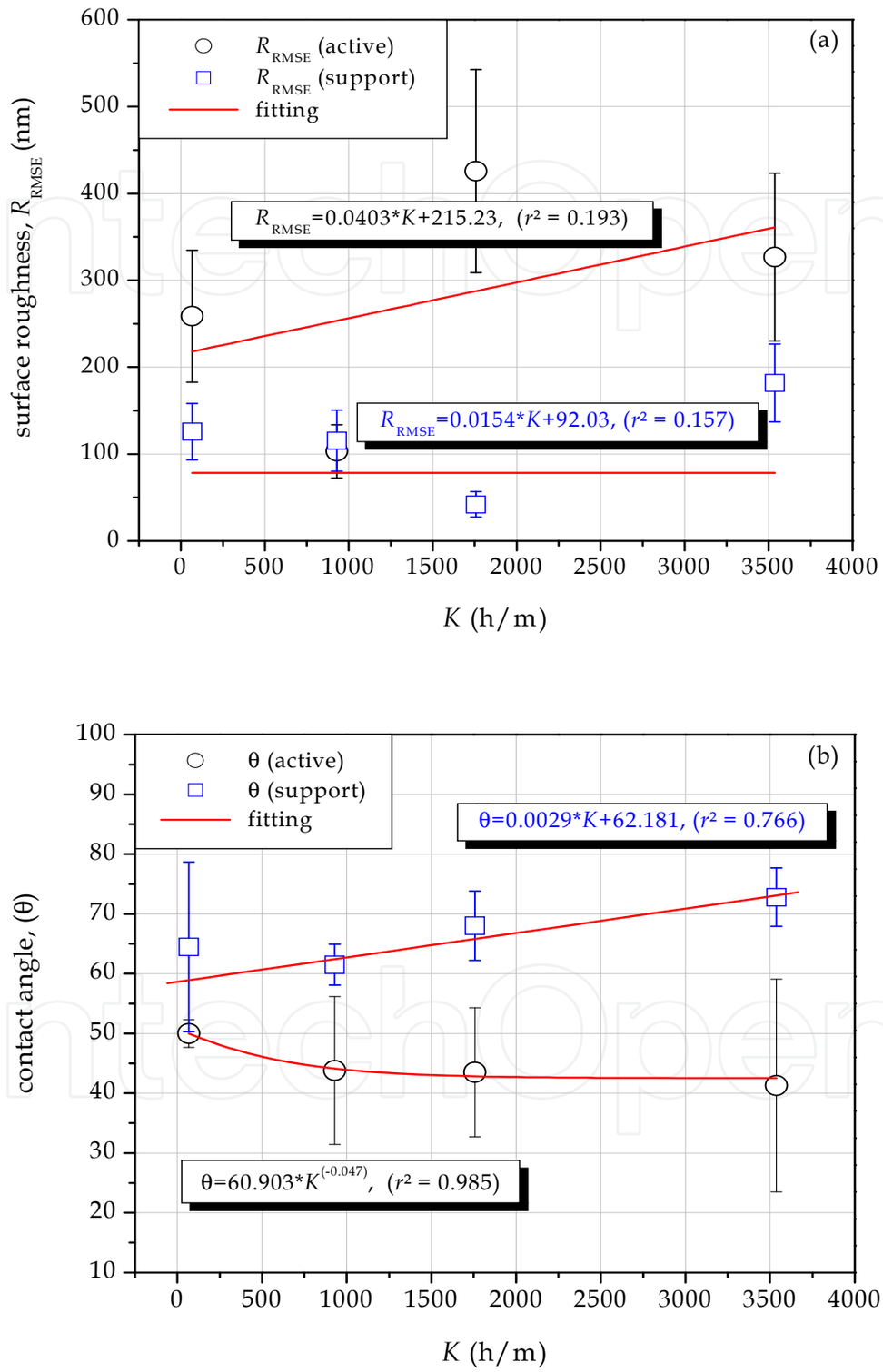

Fig. 9. Relationships of surface roughness (a) and wettability (b) to internal fouling

As can be seen from the graphs, the hydrophilicity of the active layer was the main representative for the whole system performance in second order polynomial structure. Fig. 10 proved that the performances based on net and effective driven forces realized as being under the predominant influences of external and internal foulings, respectively. The increase in the hydrophilicity yielded by the net force increase was very likely owing to the fact that soluble hydrophilic foulants increased on the surface by ionic binding or adsorption. As to the effective force increase, the hydrophilicity decrease pointed out an external fouling with the fact that soluble or insoluble hydrophobic organics were predominantly bound or attached on the surface as also supported by FTIR analyses. In FO-reverse mode, weakening in interactions among organic and inorganic solutes brought about a performance result of higher net force and excessive salt passage, whereby soluble whey organics did not notably penetrated inside the membrane's active layer. Hence, it can be said that targeting a too high rejection rate for organics, especially for ones with low-molecular weight should be seriously taken into consideration, if a FO membran devoted to the objective implementation of the process to water or wastewater containing organic substances will be improved.

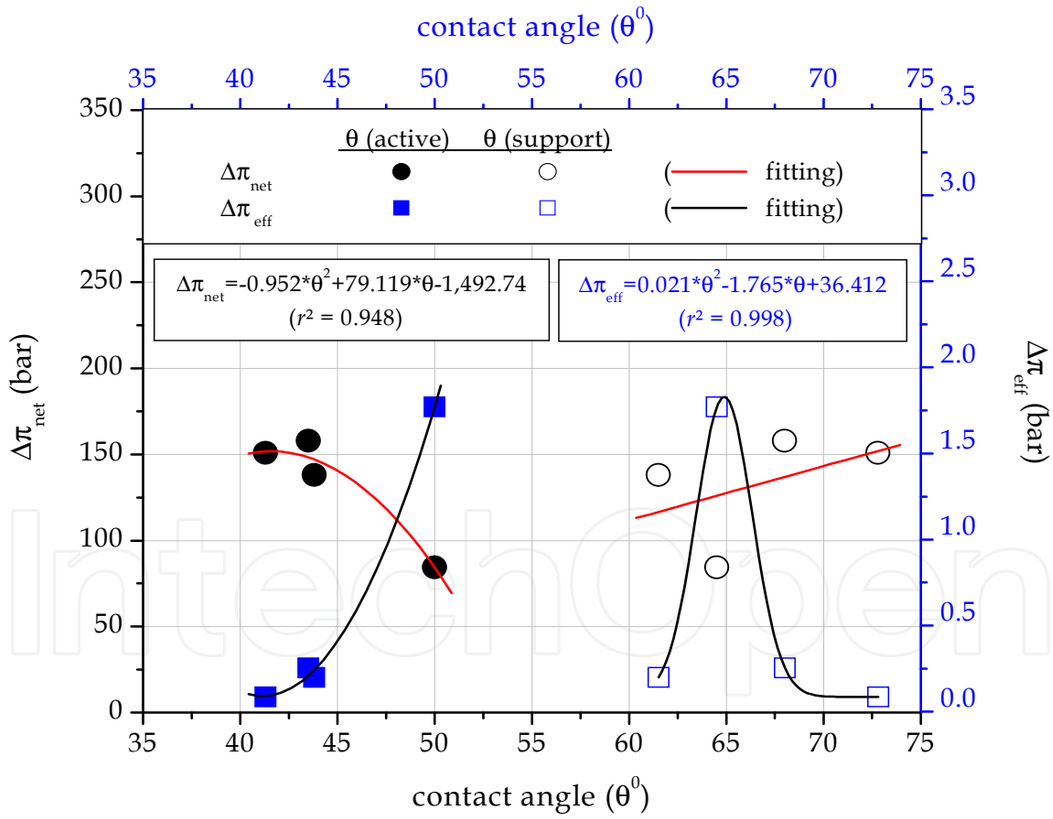

Fig. 10. Interrelationships of wettability of active and support layers with osmotically–driven forces

According to Fig. 11, the active surface became more hydrophobic as both salt flux and membrane's salt permeability increased. This concluded that the fouling on the active

surface by hydrophobic foulants in whey brought increasing of internal fouling as also supported by Fig. 9-(b). That's why, for more effective operation of a FO system involving organic-inorganic binary, the membrane has to be devised by not only achievement of high organic rejection rate but also acquirement of low hydrophobic fouling on the selective surface. To this end, it can be foreseen that the process would become more economically viable with a higher performance by means of the arrangements to be made on the active surface.

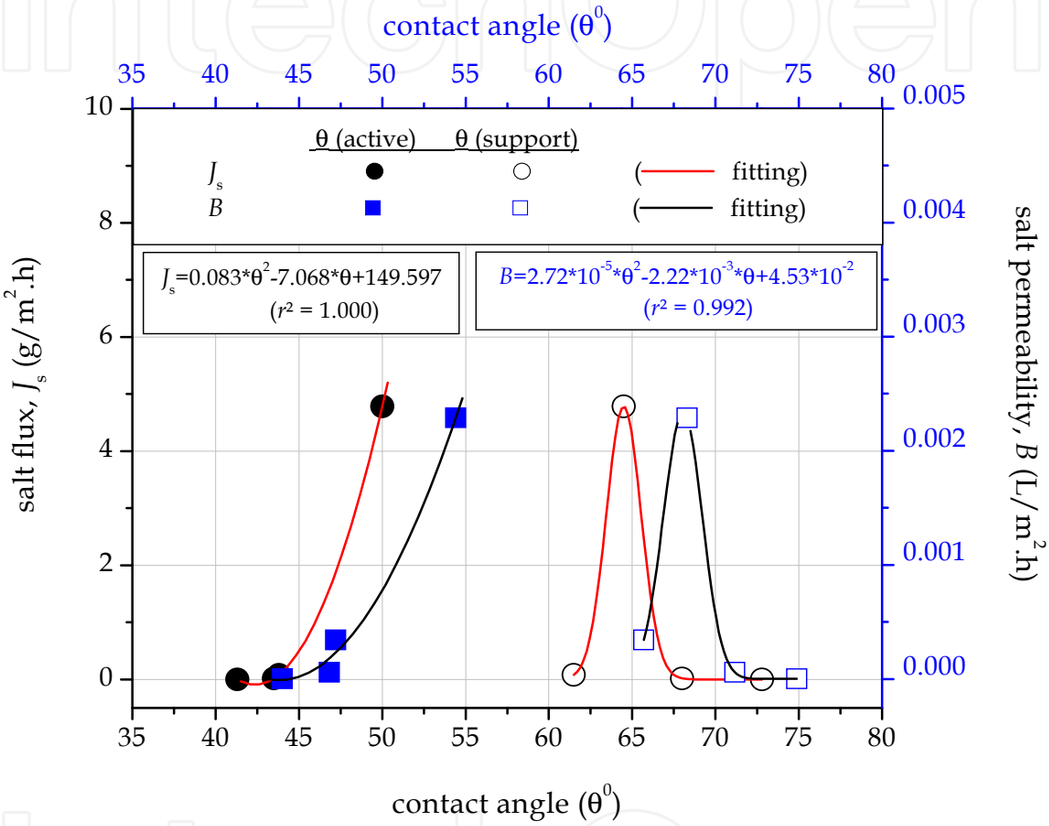

Fig. 11. Interrelationships of wettability of active and support layers with salt passage

Fig. 12 presented that each one of parameters belonging to water passage was well fitted with the active contact angles as in that of driven forces and salt passage. The decrease in the surface wettability accounted for the increase in water permeation performance of the membrane. This meant that, a FO membrane for organic-inorganic binary system have to be an optimum solution for the wettability on the active layer so that the surface should have a hydrophobic domain enough to enable as much as possible of water passage. In light of the results founded on the development of novel FO membranes, matters of fact or opinions deemed to require a thinner membrane than CTA FO membrane of about 50 μm in order to increase the corresponding effective osmotic pressure difference. It can be such that increasing membrane thickness (averagely 200-250 μm for a RO membrane) may be the major triggering factor for lower FO performance by simultaneous contribution of the increase of internal fouling and the decrease of effect of net driven force.

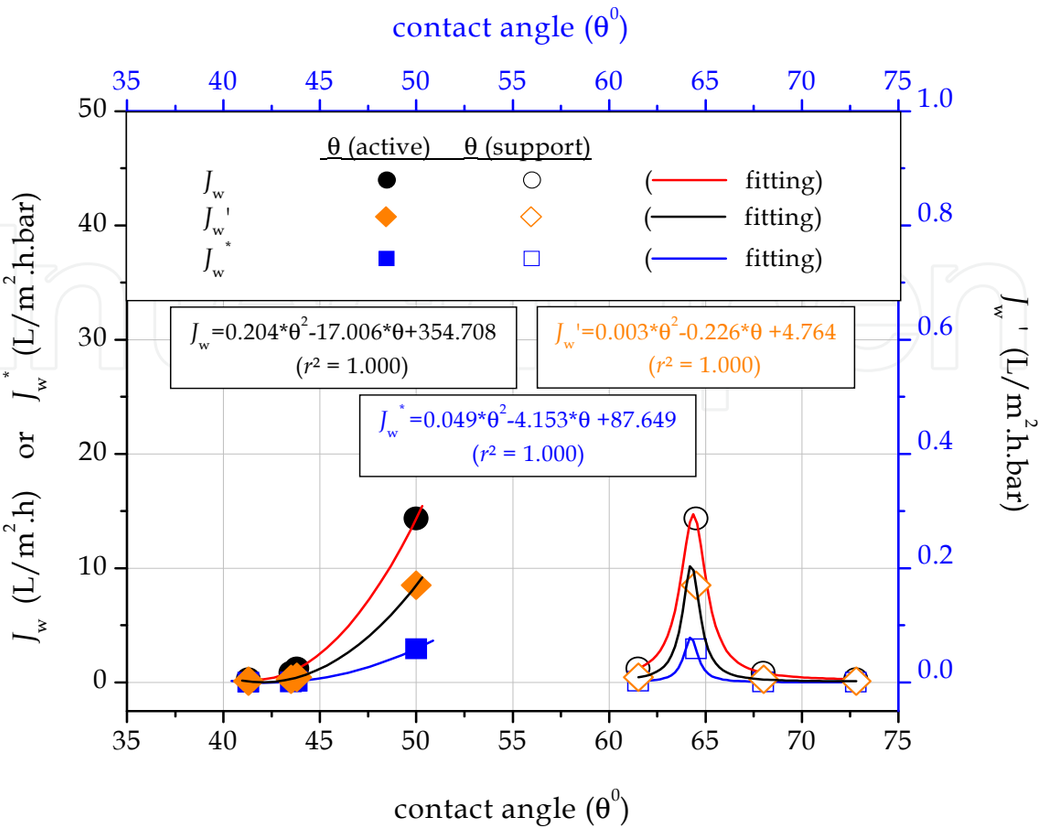

Fig. 12. Interrelationships of wettability of active and support layers with water passage

3.3.3 Performance simulation by integration of the approaches

Final performances were individually predicted for each response parameter using the second order polynomial relations obtained from the results of ex-situ-based approach (Figs. 10-12). By means of the predicted performance responses, analogical solute resistivities, K_m and K_{pe} were separately calculated for the measurable and the prevailing estimated parameters by Eqs. (14) and (15), respectively, to compare their consistency with internal fouling (actual solute resistivity, K). The consistency graph was shown in Fig. 13 in which dotted lines were the variation ranges of ±10 and ±20%. In the calculations, deviations from actual values of the responses involving driven forces, water and salt passages were determined by normalized root mean square error (Fig 14). As in modeling-based approach, the use of either the measurable or the prevailing estimated parameters in ex-situ-based approach sufficed for meaningfully describing the relationships of the fouling with the performance. The consistencies of actual and analogical solute resistivities were very close to each other. In order to estimate the performance, analogical internal foulings from the joint solution of the approaches were separately conformed by actual fouling in an acceptable variation range of almost ±10 and ±20% for the prevailing estimated and the measured parameters, respectively. In that sense, Fig. 14 presented that ex-situ-modeling-performance triple with the combination of both approaches was determined as having a capability of 10% in terms of *NRMSE* values, except for the membrane salt permeability.

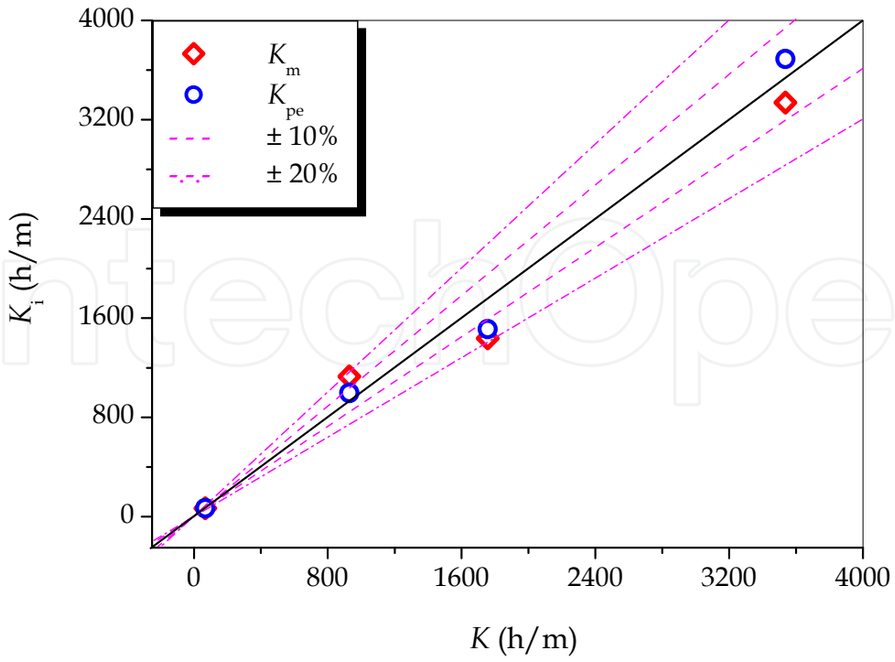

Fig. 13. Consistencies for solutions based on "*ex-situ-modeling-performance*" integration

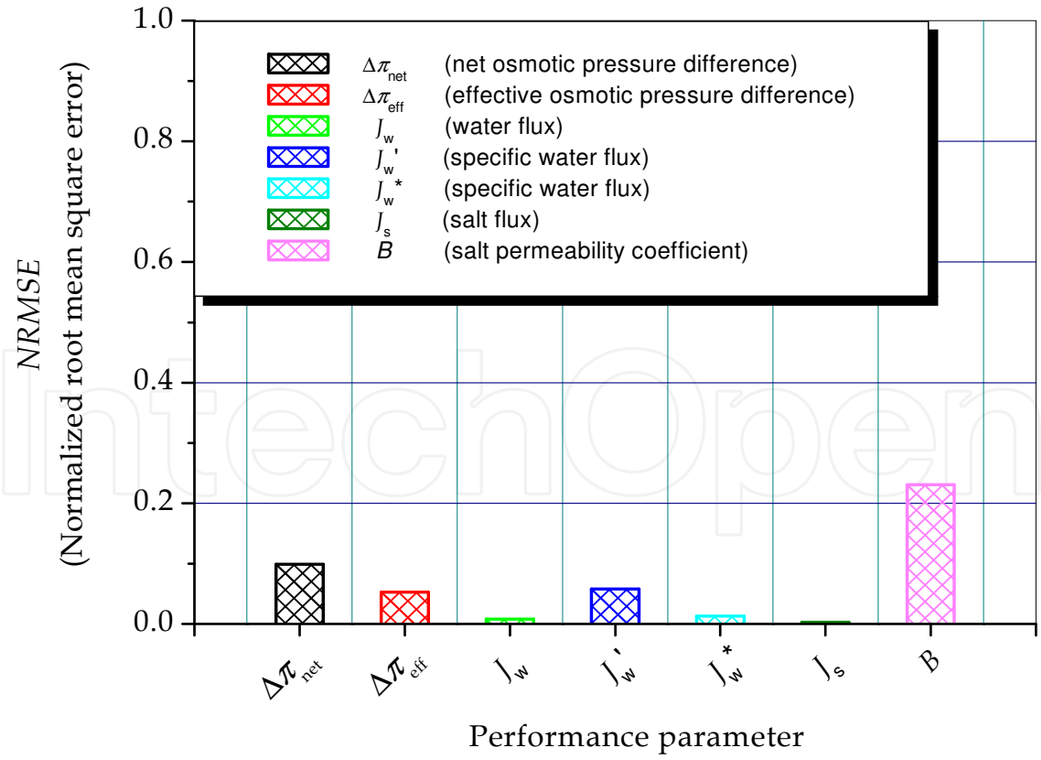

Fig. 14. Deviations from actual values of each performance response parameter with regard to the consistencies of the integrated approaches

4. Conclusion

In this study, two different approaches grounded on modeling- and ex-situ membrane characterization-based performance analysis were applied for the evaluation of performance-fouling relationships in a FO system operated as independent of the kind and orientation mode of FO and RO membranes. The prominent findings from normative interpretations together of the results related to the performance, modeling and ex-situ membrane characterizations were summarized below:

i. FO membrane operated at reverse mode exhibited better performance due to lower internal fouling compared to RO membrane. But its high salt permeability and higher increasing rate in external fouling were the main drawbacks to its more effective use.
ii. The modeling-based approach was admirably applied in interrelating internal fouling and process performance by statistical power law analyses of time-dependent and time-independent data. The approach proved that the performance restricting factors were, in decreasing order, the net pressure difference and water and salt fluxes, respectively.
iii. The ex-situ-based approach was successfully implemented in interrelating both internal-external foulings by non-linear curve-fitting and external fouling-process performance by second order polynomial curve fitting for time-independent data using the contact angle of active membrane surface. It was comprehended by the approach that the increase in external fouling increased the internal fouling. The performance of net and effective driven forces was determined to be in association with external and internal foulings, respectively.
iv. Some useful knowledge was obtained on the improvement of FO membranes by thorough evaluation of the results belonging to both the process performance analyses and the individual application of the approaches. According to the performance results, there need to be developed a novel FO membrane to be able to be employed with better salt rejection, higher water flux, and thinner membrane thickness. The modeling-based approach justified the inferences of the stand-alone performance analysis. Whereas, knowledge obtained by the ex-situ-based approach was to some extent greater. As exclusive of others two, without compromising the compatibility with net driven force, a novel FO membrane should have less external foulings on both surfaces for both organic and inorganic foulants to provide the continuity of lower internal fouling.

The integrated implementation of both approaches was also successfully carried out intended for the process simulation. The integrated approach was ascertained as a novel and progressive tool in both elucidating the performance-fouling relationships and simulating the whole performance and its components. But, the proposed methodology should amply be examined and confirmed by its experiencing in the performance predictions of full-scale membrane systems. In that sense, for the future works, testing the integrated approach for applications with real-time based on the fouling control may be offered to membrane specialists to be oriented to ex-situ-based performance simulations.

At the end of this chapter, it can be essentially said that, despite low fouling tendencies of FO membranes being easily removed by membrane cleaning, development of superior membranes having distinctive properties for various dewatering/purification applications would gain more prominence world-wide in the near future when technical and commercial inadequacies in their diversity are started to be considered more widely. By this means,

common implementations of forward osmosis as an energy efficient and environmentally-friendly desalination technology would be much more possible.

5. Acknowledgment

This study was financially supported with a national project (No: 109Y300) by the TUBITAK, the Scientific and Technological Research Council of Turkey. Authors would like to thank to the Cayirova Milk&Milk Products Inc., especially to Mr. Seyhmuz Aslan and Ms. Neslihan Genal, for the cheese whey supplement. Authors would also like to thank to Hydration Technologies Inc., and Hydranautics Inc., due to the membrane supplements.

6. References

Aaberg, R.J. (2003). Osmotic Power: A New and Powerful Renewable Energy Source, ReFocus, Vol.4, No.6, (November-December 2003), pp. 48–50, ISSN 1471-0846

American Public Health Association (AWWA), Standard Methods for the Examination of Water and Wastewater, 21th ed., Washington DC., 2005.

Aydiner, C. (2010). A Novel Approach Based on Distinction of Actual and Pseudo Resistances in Membrane Fouling: "*Pseudo Resistance*" Concept and Its Implementation in Nanofiltration of Single Solutions. Journal of Membrane Science, Vol.361, No.1-2, (September 2010), pp. 96-112, ISSN 0376-7388

Cath, T.Y.; Gormly, S.; Beaudry, E.G.; Flynn, M.T.; Adams, V.D. & Childress, A.E. (2005a). Membrane Contactor Processes for Wastewater Reclamation in Space. I. Direct Osmotic Concentration as Pretreatment for Reverse Osmosis, Journal of Membrane Science, Vol.257, No.1-2, (July 2005), pp. 85–98, ISSN 0376-7388

Cath, T.Y.; Adams, V.D. & Childress, A.E. (2005b). Membrane Contactor Processes for Wastewater Reclamation in Space. II. Combined Direct Osmosis, Osmotic Distillation, and Membrane Distillation for Treatment of Metabolic Wastewater, Journal of Membrane Science, Vol.257, No.1-2, (July 2005), pp. 111–119, ISSN 0376-7388

Cath, T.Y.; Childress, A.E. & Elimelech, M. (2006). Forward Osmosis: Principles, Applications and Recent Developments, Journal of Membrane Science, Vol.281, No.1-2, (September 2006), pp. 70–87, ISSN 0376-7388

Chen, J.C.; Li, Q. & Elimelech, M. (2004). In Situ Monitoring Techniques for Concentration Polarization and Fouling Phenomena in Membrane Filtration, Advances in Colloid and Interface Science, Vol.107, No.2-3, (March 2004), pp. 83–108, ISSN: 0001-8686

Chung, T.S.; Zhang, S.; Wang, K.Y.; Su, J. & Ling, M.M. (2011). Forward Osmosis Processes: Yesterday, Today and Tomorrow, Desalination (2011), ISSN 0011-9164, (article in press)

Cornelissen, E.R.; Harmsen, D.; De Korte, K.F.; Ruiken, C.J.; Qin, J. J.; Oo, H. & Wessels, L.P. (2008). Membrane Fouling and Process Performance of Forward Osmosis Membranes on Activated Sludge, Journal of Membrane Science, Vol.319, No.1-2, (July 2008), pp. 158–168, ISSN 0376-7388

Danis, U. & Aydiner, C. (2009). Investigation of Process Performance and Fouling Mechanisms in Micellar-Enhanced Ultrafiltration of Nickel-Contaminated Waters. Journal of Hazardous Materials, Vol.162, No.2-3, (March 2009), pp. 577-587, ISSN 0304-3894

Darton, T.; Annunziata, U.; Pisano, F.V. & Gallego, S. (2004). Membrane Autopsy Helps to Provide Solutions to Operational Problems, Desalination, vol.167, No.1-3, (March 2004), pp. 239–245, ISSN 0011-9164

Dova, M.I.; Petrotos, K.B. & Lazarides, H.N. (2007). On the Direct Osmotic Concentration of Liquid Foods. Part I. Impact of Process Parameters on Process Performance, Journal of Food Engineering, Vol.78, No.2, (January 2007), pp. 422–430, ISSN 0260-8774

Gormly, S.; Herron, J.; Flynn, M.; Hammoudeh, M. & Shaw, H. (2011). Forward Osmosis for Applications in Sustainable Energy Development, Desalination and Water Treatment, vol.27, No.1-3, (March 2011), pp. 327–333, ISSN 1944-3994

Hoek, E.M.V.; Allred, J.; Knoell, T. & Jeong, B.H. (2008). Modeling the Effects of Fouling on Full-Scale Reverse Osmosis Processes, Journal of Membrane Science, vol. 314, No.1-2, (April 2008), pp. 33–49, ISSN 0376-7388

Holloway, R.W.; Childress, A.E.; Dennett, K.E. & Cath, T.Y. (2007). Forward Osmosis for Concentration of Anaerobic Digester Centrate, Water Research, Vol.41, No.17, (September 2007), pp. 4005–4014, ISSN 0043-1354

Huang, X.; Guillen, G.R. & Hoek, E.M.V. (2010). A New High-Pressure Optical Membrane Module for Direct Observation of Seawater RO Membrane Fouling and Cleaning, Journal of Membrane Science, Vol.364, No.1-2, (August 2010), pp. 149–156, ISSN 0376-7388

Ling, M.M.; Wang, K.Y. & Chung, T.S. (2010). Highly Water–Soluble Magnetic Nanoparticles as Novel Draw Solutes in Forward Osmosis for Water Reuse, Industrial Engineering Chemistry Research, Vol.49, No.12, (May 2010), pp. 5869–5876, ISSN 0888-5885

Loeb,S.; Titelman, L.; Korngold, E. & Freiman, J. (1997). Effect of Porous Support Fabric on Osmosis Through a Loeb–Sourirajan–Type Asymmetric Membrane, Journal of Membrane Science, Vol.129, No.2, (July 1997), pp. 243–249, ISSN 0376-7388

Loeb, S. (2001). One Hundred and Thirty Benign and Renewable Megawatts from Great Salt Lake? The Possibilities of Hydroelectric Power by Pressure Retarded Osmosis, Desalination, Vol.141 No.1, (December 2001), pp. 85–91, ISSN 0011-9164

Low, S.C. (2009). Preliminary Studies of Seawater Desalination using Forward Osmosis, Desalination and Water Treatment, vol.7, No.1-3, (2009), pp. 41–46, ISSN 1944-3994

Martinetti, C.R.; Childress, A.E. & Cath, T.Y. (2009). High Recovery of Concentrated RO Brines using Forward Osmosis and Membrane Distillation, Journal of Membrane Science, vol. 331, No.1-2, (April 2009), pp. 31–39, ISSN 0376-7388

Mccutcheon, J.R.; Mcginnis, R.L. & Elimelech, M. (2005). A Novel Ammonia–Carbon Dioxide Forward (Direct) Osmosis Desalination Process, Desalination vol.174, No.1, (April 2005), pp. 1–11, ISSN 0011-9164

Mccutcheon, J.R.; Mcginnis, R.L. & Elimelech, M. (2006). Desalination by Ammonia–Carbon Dioxide Forward Osmosis: Influence of Draw and Feed Solution Concentrations on Process Performance, Journal of Membrane Science,vol.278, No.1-2, (July 2006), pp. 114–123, ISSN 0376-7388

McCutcheon, J.R. & Elimelech, M. (2006). Influence of Concentrative and Dilutive Internal Concentration Polarization on Flux Behavior in Forward Osmosis, Journal of Membrane Science, Vol.284, No.1-2, (November 2006), pp. 237–247, ISSN 0376-7388

McGinnis, R.L.; McCutcheon, J.R. & Elimelech, M. (2007). A Novel Ammonia–Carbon Dioxide Osmotic Heat Engine for Power Generation, Journal of Membrane Science, Vol.305, No.1-2, (November 2007), pp. 13–19, ISSN 0376-7388

Petrotos, K.B. & Lazarides, H.N. (2001). Osmotic Processing of Liquid Foods, Journal of Food Engineering, Osmotic Processing of Liquid Foods, Vol.49, No.2-3, (2001), pp. 201–206, ISSN 0260-8774

Tan,C.H. & Ng, H.Y. (2008). Modified Models to Predict Flux Behavior in Forward Osmosis in Consideration of External and Internal Concentration Polarizations, Journal of Membrane Science, Vol.324, No.1-2, (October 2008), pp. 209–219, ISSN 0376-7388

Tang, C.Y.; She, Q.; Lay, W.C.L.; Wang, R. & Fane, A.G. (2010). Coupled Effects of Internal Concentration Polarization and Fouling on Flux Behavior of Forward Osmosis Membranes During Humic Acid Filtration, Journal of Membrane Science, Vol.354, No.1-2, (May 2010), pp. 123–133, ISSN 0376-7388

Tu, S.C.; Ravindran, V. & Pirbazari, M. (2005). A Pore Diffusion Transport Model for Forecasting the Performance of Membrane Processes, Journal of Membrane Science, vol.265, No.1-2, (November 2005), pp. 29–50, ISSN 0376-7388

Uchymiak, M.; Rahardianto, A.; Lyster, E.; Glater, J. & Cohen, Y. (2007). A Novel RO Ex situ Scale Observation Detector (EXSOD) for Mineral Scale Characterization and Early Detection, Journal of Membrane Science, vol.291, No.1-2, (January 2007), pp. 86–95, ISSN 0376-7388

Van der Bruggen, B.; Manttari, M. & Nystrom, M. (2008). Drawbacks of Applying Nanofiltration and How to Avoid Them: A Review, Separation and Purification Technology, vol.63, No.2, (October 2008), pp. 251–263, ISSN 1383-5866

Wang, R.; Shi, L.; Tang, C.Y.; Chou, S.; Qiu, C. & Fane, A.G. (2010) Characterization of Novel Forward Osmosis Hollow Fiber Membranes, Journal of Membrane Science, Vol.355, No.1-2, (June 2010), pp. 158–167, ISSN 0376-7388

Wang, K.Y.; Teoh, M.; Nugroho, A. & Chung, T.S. (2011). Integrated Forward Osmosis–Membrane Distillation (FO-MD) Hybrid System for the Concentration of Protein Solutions, Chemical Engineering Science, Vol.66, No.11, (June 2011), pp. 2421-2430, ISSN 0009-2509

Xu, P.; Bellona, C. & Drewes, J.E. (2010). Fouling of Nanofiltration and Reverse Osmosis Membranes during Municipal Wastewater Reclamation: Membrane Autopsy Results from Pilot-scale Investigations, Journal of Membrane Science, Vol.353, No.1-2, (February 2010), pp. 111–121, ISSN 0376-7388

Xu, Y.; Peng, X.; Tang, C.Y.; Fu, Q.S. & Nie, S. (2010). Effect of Draw Solution Concentration and Operating Conditions on Forward Osmosis and Pressure Retarded Osmosis Performance in a Spiral Wound Module, Journal of Membrane Science, Vol. 348, No.1-2, (February 2010), pp. 298–309, ISSN 0376-7388

Yang, Q.; Wang, K.Y. & Chung, T.S. (2009). A Novel Dual-Layer Forward Osmosis Membrane for Protein Enrichment and Concentration, Separation and Purification Technology, Vol.69, No.3, (October 2009), pp. 269–274, ISSN 1383-5866

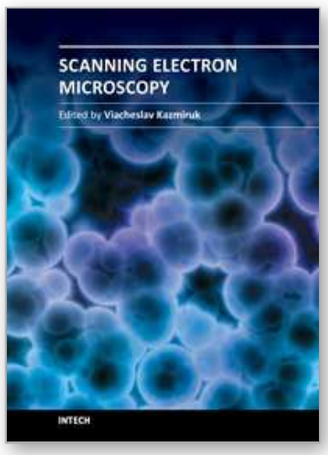

Scanning Electron Microscopy

Edited by Dr. Viacheslav Kazmiruk

ISBN 978-953-51-0092-8
Hard cover, 830 pages
Publisher InTech
Published online 09, March, 2012
Published in print edition March, 2012

Today, an individual would be hard-pressed to find any science field that does not employ methods and instruments based on the use of fine focused electron and ion beams. Well instrumented and supplemented with advanced methods and techniques, SEMs provide possibilities not only of surface imaging but quantitative measurement of object topologies, local electrophysical characteristics of semiconductor structures and performing elemental analysis. Moreover, a fine focused e-beam is widely used for the creation of micro and nanostructures. The book's approach covers both theoretical and practical issues related to scanning electron microscopy. The book has 41 chapters, divided into six sections: Instrumentation, Methodology, Biology, Medicine, Material Science, Nanostructured Materials for Electronic Industry, Thin Films, Membranes, Ceramic, Geoscience, and Mineralogy. Each chapter, written by different authors, is a complete work which presupposes that readers have some background knowledge on the subject.

InTech Europe
University Campus STeP Ri
Slavka Krautzeka 83/A
51000 Rijeka, Croatia
Phone: +385 (51) 770 447
Fax: +385 (51) 686 166
www.intechopen.com

InTech China
Unit 405, Office Block, Hotel Equatorial Shanghai
No.65, Yan An Road (West), Shanghai, 200040, China
中国上海市延安西路65号上海国际贵都大饭店办公楼405单元
Phone: +86-21-62489820
Fax: +86-21-62489821

IntechOpen